Characterization of Partially Homogenized 2x24 Ingot

Ralph T. Shuey, Thomas N. Rouns, Dhruba J. Chakrabarti, and Joanne L. Murray
Alcoa Technical Center, 100 Technical Drive, Alcoa Center, PA 15069

ABSTRACT: The possible temperatures of local eutectic melting in 2x24 alloys are defined by thermodynamics of Al-Cu-Mg, with minor reduction due to other solutes. The DSC response depends on the amount and geometry of soluble phases, and the local solute concentration near those phases. This microstructure in turn depends on the as-cast microstructure and the homogenization treatment. To better define these relationships, we quantified the constituent and solute structure, and measured DSC response, for three treatments of 2x24 ingot material. The end of solidification path is marked by Mn depletion, which is essentially unhomogenized. All constituents are clustered at grain vertices, and have about ¼ their surface area in contact with other constituents. Mostly the Fe-bearing constituents contact each other and the Cu-bearing constituents contact each other, with relatively little contact between Fe-bearing and Cu-bearing. Even after substantial reduction of DSC cal/g, the solute Cu distribution has large, long-wavelength gradients.

KEYWORDS: *Eutectic melting, homogenization, DSC, Al-Cu-Mg system, solute gradients*

Introduction

While homogenizing ingots of high-strength 2xxx alloy, temperature must be kept low enough to avoid local eutectic melting and consequent microstructural damage. However the lower the soak temperature, the slower and less complete the dissolution of soluble constituents, which can also degrade final properties. As a guide to thermal practice, differential scanning calorimetry (DSC) is done on coupons quenched from trial thermal paths. The DSC test produces in essence two numbers: the minimum temperature of local melting, and the amount of thermal energy (cal/g) taken up by the melting reaction at a standard heatup rate. The DSC temperature gives the tolerance between the thermal path and melting conditions, and also is diagnostic of the phases involved. The DSC cal/g correlates with the amount of remaining constituents.

Eutectic Local Melting in Al-Cu-Mg

We analyze homogenization of 2x24 alloys on the basis of thermodynamics and diffusion kinetics of the phases Al_2Cu (θ) and Al_2CuMg (S) in the ternary system Al-Cu-Mg [1, 2]. For the monovariant reactions involving S or θ phases individually, the solid lines in Figure 1 give the possible combinations of the Cu and Mg solute levels in the matrix contacting the intermetallic phase, and the tick marks indicate the reaction temperature. The indicated ties lines connect the composition at the reaction site with the composition outside the diffusion zone surrounding the particle. This diffusion zone, about a particle radius in thickness, sustains the dissolution reaction at the elevated temperature of either the DSC test or the homogenization soak. Next to θ-Phase the zone involves only Cu, while next to S-Phase the changes of wt% Cu and wt% Mg across the zone should be in such a ratio that the diffusion fluxes are in stoichiometric proportion. This requires

$$\frac{\Delta Cu}{\Delta Mg} = \frac{M^{Cu}}{M^{Mg}} \frac{D^{Mg}}{D^{Cu}} \approx 10$$

where M^{Mg} and M^{Cu} are the atomic masses and D^{Mg} and D^{Cu} are the atomic diffusivities. Although the two elements Cu and Mg have equal atomic proportions in S Phase, the atomic Cu enrichment of the adjacent matrix is greater because the Mg diffuses away faster.

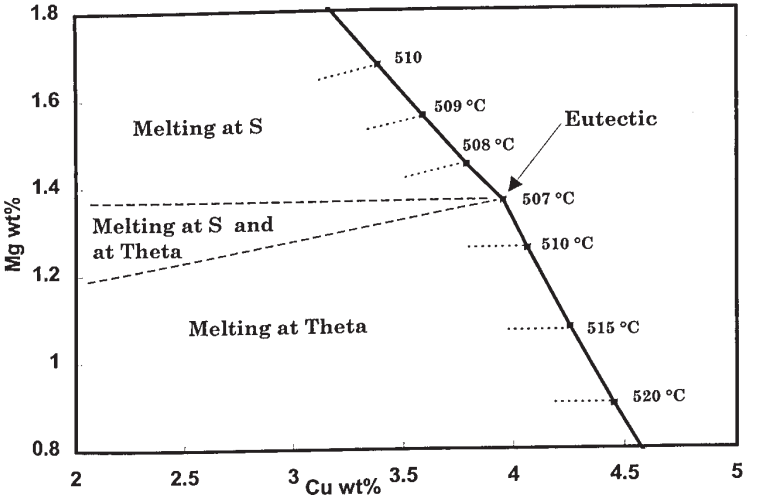

Figure 1. Local Melting Temperatures and Solute Concentrations in Al-Cu-Mg

This thermodynamic diagram relates melting temperature to solute concentrations in the matrix near the intermetallic particles. Prediction of these solute concentrations involves several factors beyond bulk composition: 1) Macrosegregation, 2) Microsegregation of elements into intermetallic phases, both insoluble and soluble, 3) Partial dissolution of soluble phases, 4) Solute gradients remaining after partial homogenization of the distribution due to microsegregation and dissolution. This investigation give quantitative examples.

Experimental Procedure

We used material from the center of a 16" ingot of 2x24 with melt wt% composition Si=0.067, Fe=0.056, Cu=4.02, Mg=1.36, Mn=0.51. We treated and tested three coupons as shown in Table 1. The microstructure and constituents in these partially homogenized samples were mapped by SEM backscatter and X-ray spectra, at several different scales. Then solute concentration was mapped and profiled by microprobe on sample C only.

Table 1. Thermal Treatments and DSC Results.

	Thermal Treatment	Temp	cal/g
A	16 hr heatup to 499°C	505°C	1.31
B	16 hr heatup to 490.5°C, 20 hr soak	508°C	0.47
C	16 hr heatup to 490.5°C, 20 hr soak with rise to 493.3°C	505°C	0.16

Microstructure

Grains are distinguished by electron channeling contrast, i.e., the dependence of backscatter intensity on crystallographic orientation. We measured mean-intercept grain size 160 micron. The constituent particles are predominately located where three or more grains come together, i.e., at grain vertices. Boundaries between just two grains are often free of constituents, suggesting the

contact was made at a high angle to the solidification front. The termination of the solidification sequence is marked by narrow Mn-depletion zones. These are nearly as cast, because Mn diffuses less than 1 micron during our heat treatment, while the zones are 5-10 micron wide. They can be mapped either by the Mn X-ray lines or by reduced backscatter intensity. The Mn-depletion zones envelope all the constituents clustered at grain vertices, and also form a network of interdendrite walls within grains. These intragranular solidification boundaries are marked by "island chains" of constituents finer and more isolated than those at grain vertices. From more detailed study of similar ingot we believe the mean intercept spacing of the Mn-depletion zones to be about 70 micron.

Constituents

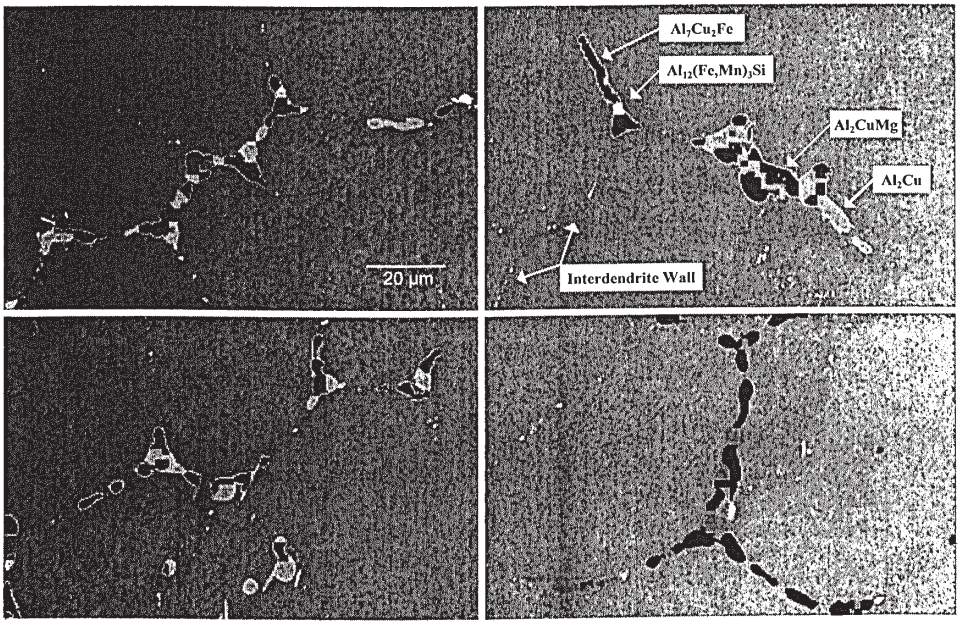

Figure 2. Constituents in Selected Clusters, Sample B 1μ grid

Table 2. Constituent Geometry in Clusters Selected from all Samples, 1μ Grid.

	Vol%	Mean Intercept	Matrix Contact	Constituent Contact, x random			
				Al_7Cu_2Fe	$Al_{12}(Fe,Mn)_3Si$	θ phase	S phase
Al_7Cu_2Fe	1.1%	8.5μ	73%		18	5	4
$Al_{12}(Fe,Mn)_3Si$	0.5%	6.6μ	73%	14		4	2
θ phase	1.3%	5.8μ	67%	4	3		10
S phase	2. 9%	7.2μ	80%	3	2	12	

We classified constituent phases on 4 frames per sample, as shown in Figure 2, using SEM X-ray spectra on a 1μ grid. We determined vol% by counting grid points, and area per volume of various contacts by counting intercepts on all grid lines. Table 2 gives the stereologic results averaged over all three samples. The vol% in Table 2 are not representative of the whole sample, as the frames were selected for soluble constituents; Table 3 gives more representative vol%. Minor constituent $Al_{20}Cu_2Mn_3$ was detected, but is too sparse to quantify. For all constituents the mean

intercept size is of order 6-8μ, and only 3/4 of the surface area is in contact with the matrix. The remainder of Table 2 shows the contact area with other constituents, relative to random. For each row, the number given is a dimensionless ratio: percentage of its area contacted by the constituent in the column, divided by the volume percent of that constituent in the column. In addition to the clustering at grain vertices, indicated by factors typically 4x, there is an affinity of the two Fe-bearing phases for each other, and likewise an affinity between the soluble θ and S phases. This contact affinity reflects proximity on the solidification path.

To get the absolute amounts of constituent phases, we used randomly selected frames. The three levels of effort in Table 3 are: 1) 5 frames per sample, 2) 40 frames per sample, and 3) discarding from the 40-frame data those points at which none of the alloying elements was more than 5 standard deviations above background, on the assumption that the beam largely missed the constituent. About 8% of the data were so discarded. The three levels give increasingly plausible results for the absolute percentages of constituents.

Table 3. Vol% Constituents in Random Frames, 3μ grid.

	5 frames			40 frames			40 frames-8% misses		
	A	B	C	A	B	C	A	B	C
Fe-bearing	0.552	0.34	0.307	0.323	0.349	0.396	0.466	0.436	0.439
θ-Phase	0.289	0.173	0.0	0.417	0.242	0.139	0.308	0.185	0.104
S-Phase	0.126	0.103	0.006	0.155	0.209	0.055	0.122	0.179	0.048
Total	0.966	0.615	0.313	0.895	0.800	0.590	0.895	0.800	0.590

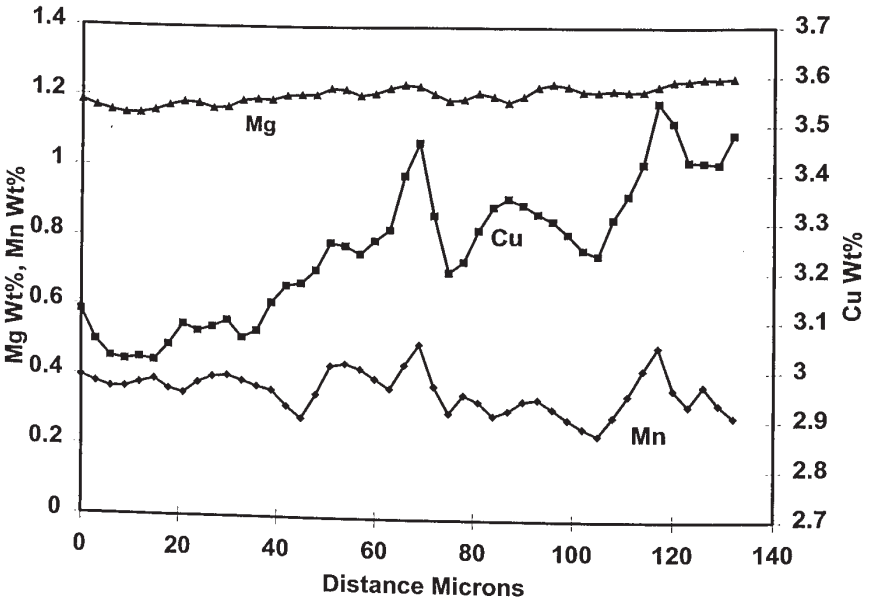

Figure 3. Composition Profile Across Grain Boundary, Sample C.

Solute

The most interesting microprobe results pertain to solute gradients on the scale of the spacing between constituent clusters. Figure 3 shows a profile centered on a grain boundary. In section it is perpendicular to the boundary, but we cannot know the 3D orientation. The mean level of Mn is neither as low as in the Mn-depletion zones (0.2 wt%), nor as high as in the peak adjacent to the Mn-depletion zones (0.6 wt%), The short-wavelength fluctuations in Mn and Cu are correlated, because the microprobe includes dispersoid $Al_{20}Cu_2Mn_3$ along with the solute. In addition there is a large long-wavelength gradient of Cu. Solute Mg is nearly homogenized, but has a small long-wavelength gradient in the same sense as the Cu gradient. Figure 4 is crossplot of Cu and Mn a long profile traversing several grains while avoiding constituent clusters. In the right-hand part of Figure 4 we estimate solute Cu by assuming that all Mn above 0.2 wt% is in $Al_{20}Cu_2Mn_3$. It appears that solute Cu is positively correlated with Mn. This may be because until the end of the solidification path solute Cu and solute Mn are positively correlated; it is only at the interdendrite wall that they become strongly anticorrelated.

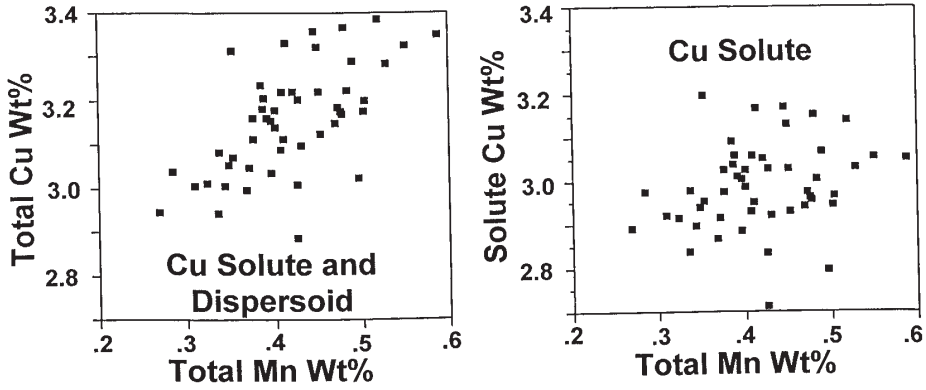

Figure 4. Correlation of Cu and Mn on Long Profile, Sample C.

Interpretation of DSC

We have extensive experience with DSC tests on 2x24 alloys quenched from possible homogenization treatments [3,4]. With both θ-Phase and S-Phase constituents present, the practical limitation on soak temperature is the melting reaction at these phases in contact. The observed temperatures are in the range 504-506°C. We believe most of the drop from the invariant eutectic temperature of 507°C in the Al-Cu-Mg system is due to Si in solid solution. Microprobe maps of Si distribution show a significant segregation from the matrix into all constituents, including θ-Phase and S-Phase. Therefore solute Si is enhanced in the diffusion zone next to the soluble particles. In the quaternary system Al-Cu-Mg-Si [1], the monovariant melting reaction at θ-Phase and S-Phase in contact extends from the ternary eutectic at 507°C down to the quaternary invariant eutectic (with Mg_2Si) at 503°C.

In 2x24 alloys with higher Si than the composition tested here, there is some constituent Mg_2Si as cast. Until the Mg_2Si is dissolved, the lowest melting temperature is the reaction involving θ-Phase, S-Phase, and Mg_2Si. Often DSC temperatures are about 1°C below the 503°C invariant temperature in the Al-Cu-Mg-Si quaternary, possibly due to other elements in solid solution.

The amount of S-Phase in Sample B (Table 3 and Figure 5) is anomalously large relative to a trend from samples A to C. Likewise the reported temperature from DSC testing (Table 1) is higher than possible for reaction simply at θ-Phase and S-Phase in contact, but not as high as we normally observe when all θ-Phase has been dissolved. We suppose that the large amount of melting at isolated S-phase has distorted the automated picking of the endothermic onset due to melting at θ-Phase and S-Phase in contact. We have no firm explanation for the anomalous S in Sample B.

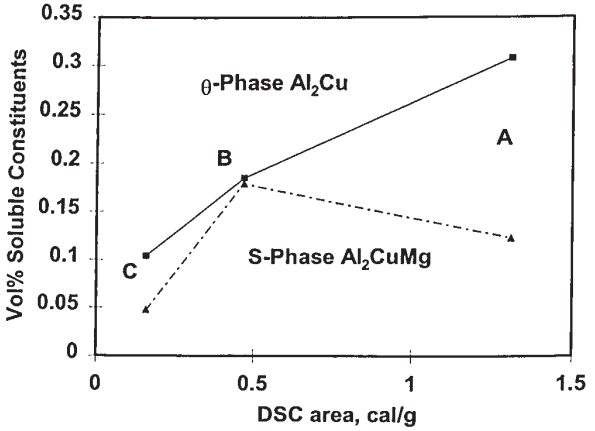

Figure 5. Crossplot of DSC Area and Vol% Soluble Constituents.

In principle the amounts and geometry of the soluble constituents determine the DSC response, but we don't have a practical algorithm. One datum towards such a calculation is the crossplot in Figure 5 of measured DSC area and measured constituent amounts. Discounting S-Phase in Sample B as just discussed, we have a quantitative example of how the DSC area for the reaction involving θ-Phase and S-Phase in contact decreases as the amounts of both soluble constituents decrease. Interestingly the S/θ ratio is nearly the same in Samples A and C, which might be attributed to the intimate contact of the two phases (Table 2) as well as the proximity of their solvi.

1 J. L. Murray, J. Chim Phys 90 (1993), 151.

2 R. T. Shuey, J.P. Suni, R. D. Doherty, and D. J. Chakrabarti, Proc ICAA5, Grenoble (1996), 735.

3 D. J. Chakrabarti and J. L. Murray, Proc ICAA5, Grenoble (1996), 177.

4 D. J. Chakrabarti, unpublished Alcoa reports.